

# Focused Ultrasound Neuromodulation of Human *In Vitro* Neural Cultures in Multi-Well Microelectrode Arrays

Ruixing Liang<sup>1,2</sup>, Griffin Mess<sup>2,3</sup>, Joshua Punnoose<sup>2,3</sup>, Kelley M. Kempfski Leadingham<sup>2,3</sup>, Constantin Smit<sup>2,3</sup>, Nitish Thakor<sup>1,4</sup>, Christa W. Habela<sup>3</sup>, Betty Tyler<sup>3</sup>, Yousef Salimpour<sup>3</sup>, Amir Manbachi<sup>1,2,3,4,5,6</sup>

<sup>1</sup>Electrical and Computer Engineering, Johns Hopkins University <sup>2</sup>HEPIUS Innovation Laboratory, Johns Hopkins University School of Medicine <sup>3</sup>Neurosurgery, Johns Hopkins University School of Medicine <sup>4</sup>Biomedical Engineering, Johns Hopkins University School of Medicine <sup>5</sup>Mechanical Engineering, Johns Hopkins University <sup>6</sup>Anesthesiology and Critical Care Medicine, Johns Hopkins University School of Medicine

## Corresponding Author

Amir Manbachi

amir.manbachi@jhu.edu

## Citation

Liang, R., Mess, G., Punnoose, J., Kempfski Leadingham, K.M., Smit, C., Thakor, N., Habela, C.W., Tyler, B., Salimpour, Y., Manbachi, A. Focused Ultrasound Neuromodulation of Human *In Vitro* Neural Cultures in Multi-Well Microelectrode Arrays. *J. Vis. Exp.* (2024), e65115, doi:10.3791/65115 (2024).

## Date Published

May 3, 2024

## DOI

10.3791/65115

## URL

jove.com/video/65115

## Introduction

Focused ultrasound (FUS) is a promising neuromodulation modality that enables noninvasive stimulation at centimeter-level depths with sub-millimeter resolution<sup>1,2,3</sup>. Despite these strengths, the clinical impact of FUS is limited, in part due to a lack of knowledge regarding its mechanism of action. Without a solid theoretical foundation, researchers and clinicians face difficulties in tailoring the therapy to

meet the specific needs of individual patients under varying conditions. A prominent theory proposed by Yoo et al.<sup>4</sup> suggests that mechanosensitive ion channels are responsible for neuron activation. However, this theory fails to explain FUS activation in human brain neurons, which lack these channels<sup>5</sup>. This ambiguity limits the utilization of FUS in

## Abstract

The neuromodulatory effects of focused ultrasound (FUS) have been demonstrated in animal models, and FUS has been used successfully to treat movement and psychiatric disorders in humans. However, despite the success of FUS, the mechanism underlying its effects on neurons remains poorly understood, making treatment optimization by tuning FUS parameters difficult. To address this gap in knowledge, we studied human neurons *in vitro* using neurons cultured from human-induced pluripotent stem cells (HiPSCs). Using HiPSCs allows for the study of human-specific neuronal behaviors in both physiologic and pathologic states. This report presents a protocol for using a high-throughput system that enables the monitoring and quantification of the neuromodulatory effects of FUS on HiPSC neurons. By varying the FUS parameters and manipulating the HiPSC neurons through pharmaceutical and genetic modifications, researchers can evaluate the neural responses and elucidate the neuro-modulatory effects of FUS on HiPSC neurons. This research could have significant implications for the development of safe and effective FUS-based therapies for a range of neurological and psychiatric disorders.

the clinic, as it precludes the tuning of FUS parameters to optimize treatment outcomes.

Prior related studies have employed a range of approaches to investigate the physiological mechanisms underpinning FUS and to determine the optimal stimulation parameters. A crucial step in this process involves monitoring neuronal responses as feedback, which can be achieved through methods involving ion-gate monitoring, such as calcium ion imaging<sup>4</sup>, optical imaging<sup>1</sup>, and *ex vivo* electrophysiological recording (e.g., electromyography<sup>6</sup> or skin-nerve electrophysiology<sup>7</sup>). However, most of these studies use non-human neurons or *in vivo* approaches, which can introduce additional variances due to sub-optimal controls. In contrast, using electrodes to measure neuronal signals in *in vitro* human-induced pluripotent stem cell (HiPSC) neurons offers more sensitive measurements and greater control over the experimental environment. In this work, an *in vitro* system has been developed using micro-electrode arrays (MEAs) to measure the electrical responses of HiPSC neurons following FUS stimulation, as shown in **Figure 1**. This system empowers researchers in the community to monitor neuronal responses when varying the ultrasound parameters (e.g., frequency, burst length, intensity). Additionally, this system enables a high level of control of the neuronal sensitivity to physical stimuli (e.g., temperature, pressure, and cavitation)<sup>8,9</sup>, as the neurons' ion channel functionality can be manipulated genetically and pharmaceutically (e.g., using gadolinium to inhibit ion channels)<sup>10,11,12</sup>. This molecular-level control may help to elucidate the mechanisms behind the neuromodulatory effects of FUS.

## Protocol

### 1. Preparation of materials

1. Aspirate the culture medium, and use it to fill a single well in a 24-well neuron culture plate with embedded MEA (**Figure 2A**). Culture and induce the neurons following the published protocol by Taga et al.<sup>13</sup>.
2. Sterilize the parafilm interface, the rubber band, and the FUS cone with its rubber membrane using 70% ethanol for 10 min, and place them in the fume hood for later assembly.
3. Degas 300 mL of deionized water and 50 mL of coupling gel. Centrifuge the water and gel at 160 x *g* for 5 min to avoid inducing cavitation within the coupling medium.

**NOTE:** The original source of the HiPSCs is from GM01582 and CIPS cell lines. On average, a density of  $5 \times 10^4$  motor neurons and  $2.5 \times 10^4$  astrocytes per well can be achieved<sup>14</sup>.

### 2. Connection and setup of the peripherals

1. Secure the FUS cone to the transducer using screws, and seal the cone with a flexible rubber membrane in a ventilated sterile hood. Fill the cone with the degassed and deionized (DG-DI) water from step 1.3, and ensure the absence of bubbles in the cone to avoid cavitation.
2. Use a customized threaded rod to secure the 3D-printed holder to a frame (**Figure 2B**). Position the frame such that the head of the FUS transducer is over the well that will be stimulated.
3. Use a rubber band to secure parafilm over the well on the 24-well MEA plate containing the medium and the HiPSCs.

4. Prepare the FUS system by connecting the ultrasound transducer's back-end driver electronics, in this case, the transducer power output (TPO; **Figure 3A**), to a 100-240 V power outlet (**Figure 3B**, Connection 6) and connecting the matching network to the TPO and the FUS transducer (**Figure 3B**, Connection 1 and Connection 2, respectively). The matching network ensures efficient electrical coupling between the transducer and the TPO.
5. Connect the MEA system to a power outlet (100-240 V) (**Figure 3B**, Connection 5). Connect the MEA system synchronization port to the TPO (**Figure 3B**, Connection 3). This connection will synchronize the data acquisition by the MEA system with the FUS stimulation.
6. Place the 24-well MEA plate in the MEA system, and remove the lid to enable direct contact between the transducer and the well. Place the transducer 5-10 mm above the well plate to allow room for the degassed coupling gel, as described in step 3.2 (**Figure 3A** and **Figure 2B**).

### 3. Stimulation and neuronal signal acquisition

1. Set the FUS parameters on the TPO control panel (**Table 1**).
2. Apply the coupling gel on top of the parafilm, and lower the FUS transducer into the coupling gel, ensuring contact with the gel with minimal air bubbles (**Figure 2A**).
3. Start the MEA system recording by clicking on the **Start** button on the user interface.
4. Start the FUS sonication by pressing the bottom right button on the TPO (**Figure 3A**, Label 7), and wait at least 5 min between each round of sonication to allow the neurons to return to a baseline state.

5. Use the trigger pulse generated by the FUS system to align the FUS stimulation sequence to the MEA recording (**Figure 3B**, Connection 3).

### 4. Data processing and analysis

1. Transfer the data from the MEA system to the computer using a USB connection (**Figure 3B**, Connection 4). Start this by clicking on the **Experiment Set Up** panel. Next, choose the data type one wishes to record. In this case, raw spikes are recommended. Finally, name the file, and select the desired location within the disk drive to complete the transfer.

**NOTE:** The following steps can be performed by running the released Python script in <https://github.com/Rxliang/FUSNeuromod>.

2. Read in the data from each of the 16 electrodes.
3. Apply a Butterworth bandpass filter with a 5 Hz to 3 kHz bandwidth with a Butterworth order of 8.

**NOTE:** To optimize these values, it is crucial to take into account the firing rate of the specific cells and the number of cells involved. By multiplying these 2 values, one can estimate the overall firing rate of the cell population in the experiment.

4. Apply a Gaussian filter with  $\sigma = 3$  to smooth the signal.
 

**NOTE:** The parameter could be optimized based on the recommended values from the MEA system, as excessive smoothing may result in data distortion after acquisition, and too little smoothing would introduce unwanted noise.
5. Set a threshold to detect the potential spikes as 5 times the standard deviation of the Gaussian-smoothed signal.
6. Compute the firing rate by dividing the number of spikes registered in a 50 ms window across all 16 channels by

the length of the window (i.e., 50 ms). Shift the window along the signal to the next frame, and repeat the firing rate calculation (**Supplementary Figure 1**).

- Analyze the signal by reading the FUS sonication time from the transferred data based on the change in the firing rate associated with the FUS.

## 5. Multi-well MEA plate cleaning and reuse

- Once the experiments are complete, use a pipette to carefully remove the medium from the wells in the multi-well plate, taking care to avoid the electrode surface.
- Add 2 mL of DG-DI water per well. Aspirate and repeat once.
- To dislodge any cells and debris, add a mixture of 1 g of enzymatic detergent Terg-A-Zyme with 10 mL of sterile DG-DI water (0.3 mL per well) to the plate. Leave it to incubate overnight at room temperature (RT).
- The following day, remove the solution from the wells, and rinse them with 1 mL of sterile DG-DI water.
- Incubate the multi-well plate for 5-7 min, and aspirate. Repeat this step 5 times.
- Add 0.5 mL of sterile DG-DI water per well. Record the baseline of the cleaned multi-well plate to validate that the MEA plate is clean. A cleaned plate should exhibit Gaussian noise patterns with low intensity values.
- Store the cleaned multi-well plate at 4 °C until it is ready to be used again. Change the water the MEAs are stored in at least once per month.

## Representative Results

In summary, we present a protocol that enables *in vitro* FUS neuromodulation monitoring using neurons cultured from

HiPSCs. The overall system platform to stimulate HiPSC-induced neurons and record the corresponding electrical responses for analysis is outlined in **Figure 1**. This study focuses on the FUS stimulation of neurons and recording the electrical responses in an MEA system, as shown in **Figure 2**. The peripheral components of the FUS and MEA systems and their connections are illustrated in **Figure 3**.

The characterization of the focal point is performed prior to the neuronal experiments to ensure the bottom of the well is fully covered by the FUS focal point. The visualization of the focal spot on thermochromic sheets, as shown in **Figure 4**, should be performed to evaluate the FUS system. Following focal spot characterization, the post-processing steps, including filtering, thresholding, and calculating the firing rate, should be performed, and these are summarized in **Figure 5** and **Figure 6**. These steps are essential to retrieve useful signals by filtering noise from the environment and, thus, to gain insight into the neuronal activity changes caused by FUS. The Raster plots in **Figure 6A-B** show the detected spikes in each channel. As the entire bottom of the well is within the focal point of the FUS transducer, it is expected that the FUS should alter the firing rate across all the electrodes. This change in firing rate is visualized in the firing rate plot shown in **Figure 6C**, which shows that the chosen stimulation parameters resulted in an increase in the neuronal firing rate. Specifically, the pre-FUS (i.e., baseline) firing rate was 140 Hz  $\pm$  116.7 Hz, while the post-FUS firing rate was 786 Hz  $\pm$  419.4 Hz with continuous-wave FUS. Additionally, **Figure 6C** shows how altering the FUS parameters (e.g., using pulsed-wave FUS instead of continuous-wave) can alter the magnitude of change in the firing rate, as well as change the amount of time before the neurons return to their baseline state. Low-intensity focused ultrasound (LIFU) does not cause significant warming of cultures, especially when

compared to high-intensity focused ultrasound, which intends to achieve thermal lesion. The lack of clinically impactful temperature change is supported by theoretical calculations and simulations (**Supplementary Figure 2**). Even in extreme cases of the experimental FUS parameters listed in **Table 1**, only a minimal increase in temperature could be observed of approximately 0.04 °C.

The use of a firing rate plot enables the quantification of the neuromodulatory effects of FUS and can be used to differentiate between excitatory and inhibitory responses. A significant advantage of the multi-well MEA plate is that it can be reused multiple times to study varying neuronal states and stimulation parameters in a high-throughput manner.

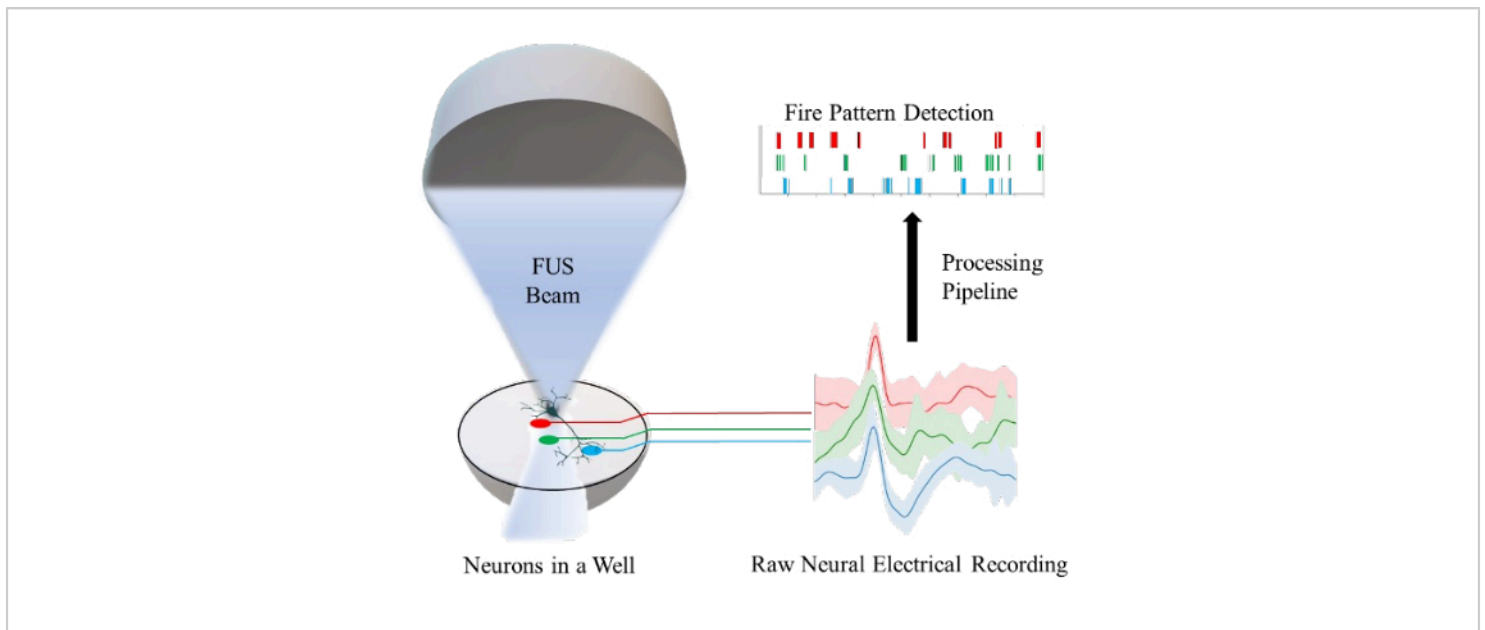


**Figure 1: Overview of the *in vitro* platform for the focused ultrasound (FUS) neuromodulation of neurons in a well and the measurement of their neuronal activity using a microelectrode array.** Each electrode (red, green, and blue lines) records from a population of neurons within a single well. A processing pipeline is implemented to convert the raw neuronal electrical recordings into the detection of neuronal firing patterns. [Please click here to view a larger version of this figure.](#)

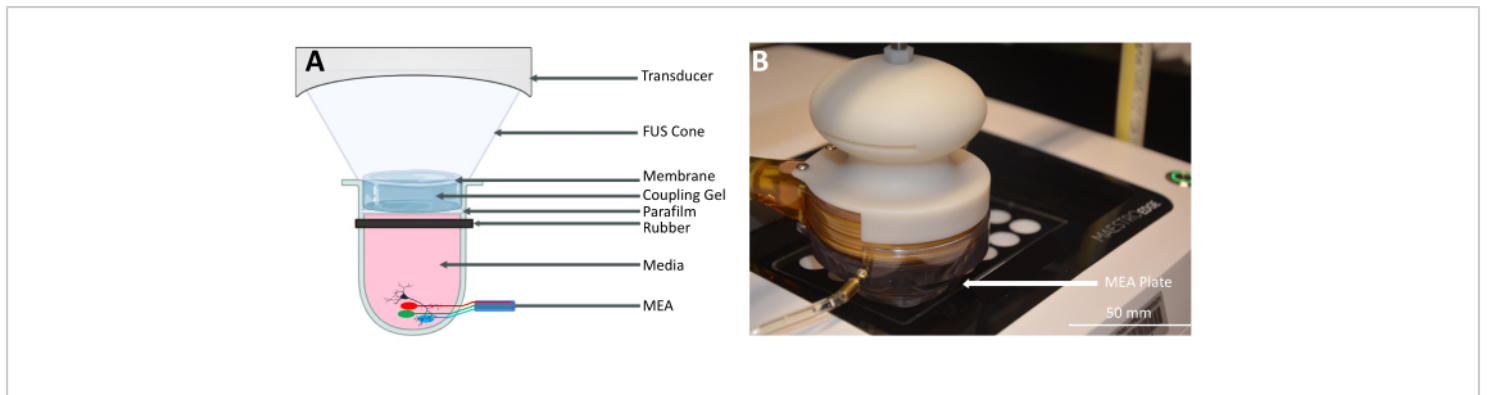


**Figure 2: FUS neuromodulation with a multi-well microelectrode array (MEA).** (A) Schematic of the setup for FUS neuromodulation with a multi-well MEA. The acoustic waves generated by the FUS transducer propagate through an FUS cone filled with degassed water and are coupled using ultrasound gel. The parafilm is secured to the well using a rubber band to prevent contamination. The MEA plate sends electrical recordings from the neurons to the MEA system. (B) A photograph of the FUS transducer on the multi-well plate contained in the MEA system. [Please click here to view a larger version of this figure.](#)

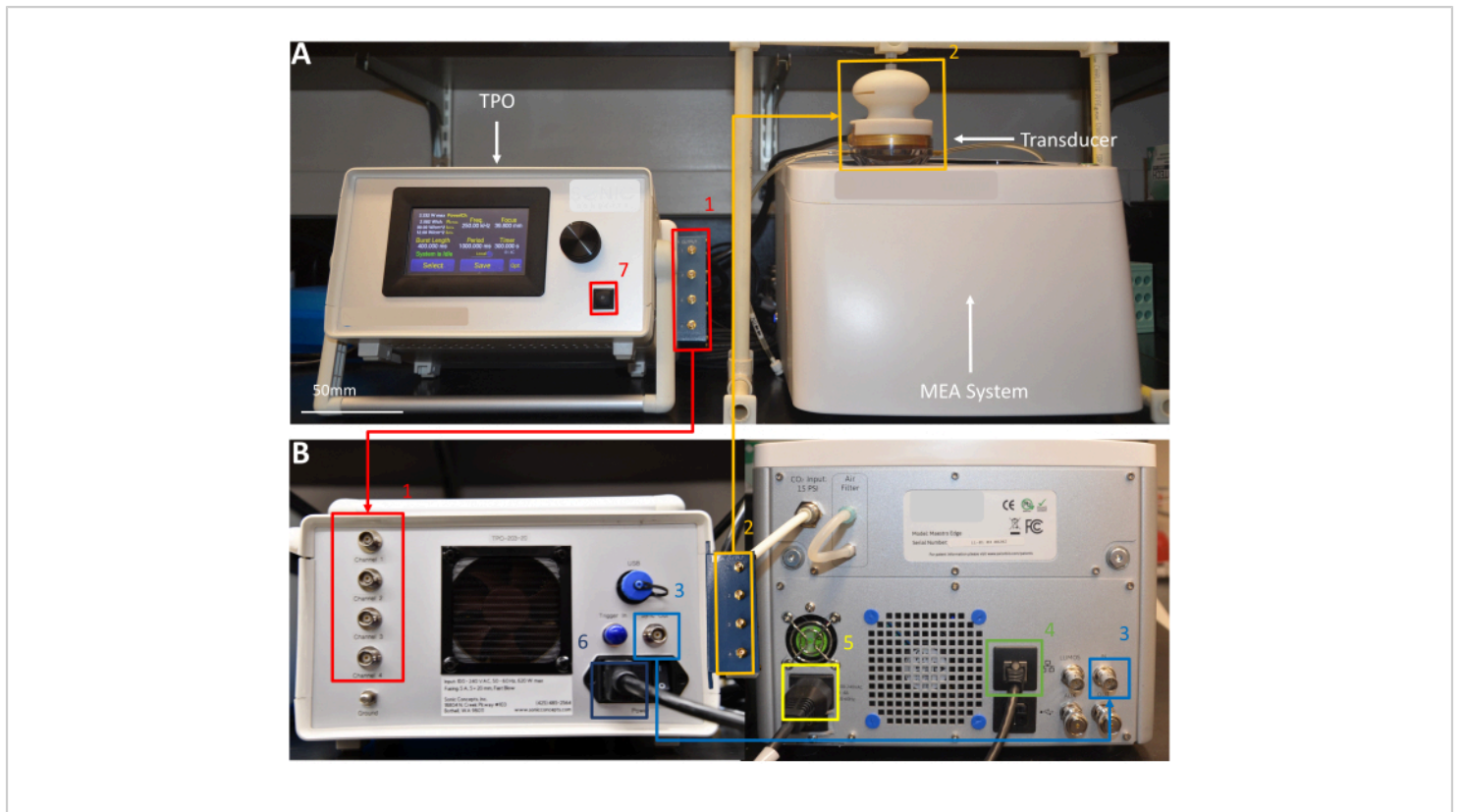


**Figure 3: *In vitro* platform setup.** (A) The front of the *in vitro* platform setup. The transducer power output (TPO; left) is used to program the FUS parameters. The MEA system (right) records electrical activity from the neurons in the well plate, which are neuromodulated by the FUS transducer. (B) The back of the *in vitro* platform setup with connections from the matching network (1) to the TPO and (2) to the transducer. (3) The connection from the MEA system to the TPO synchronizes the data acquisition. (4) The connection from the MEA system to the computer for data transfer. (5) The power connection to the MEA system. (6) The power connection to the FUS system. (7) The sonication button. [Please click here to view a larger version of this figure.](#)

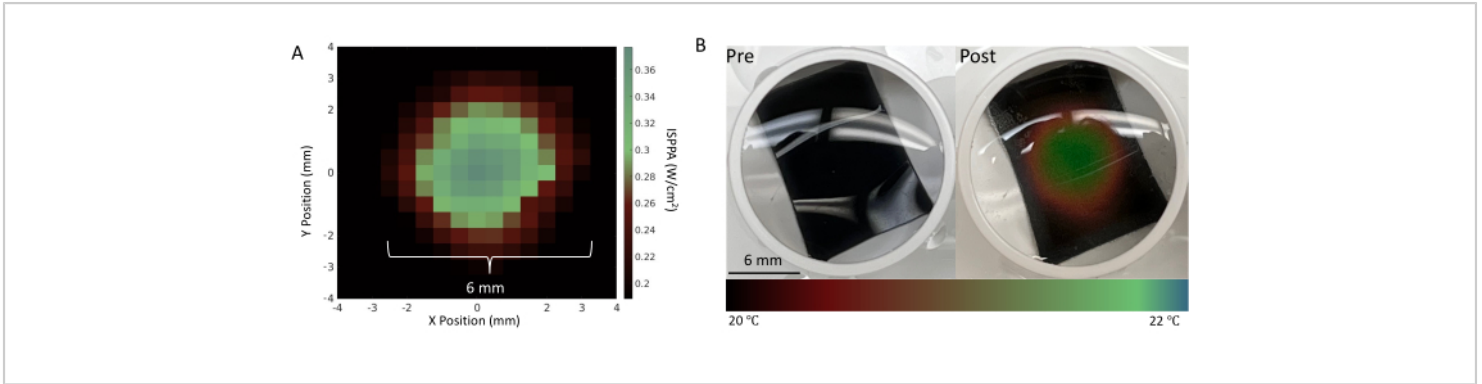


**Figure 4: Characterization of the FUS transducer.** (A) A pressure map of the focal spot using the FUS parameters detailed in **Table 1** measured by the AMPLITUDE system<sup>15</sup>. (B) Pre- and post-sonication of a thermochromic sheet placed at the bottom of a well using the experimental setup shown in **Figure 3**. The thermochromic sheet changes color in response to temperature changes, which provides a visual validation of successful stimulation at the location of the neurons. The maximal spatial-peak pulse average intensity ( $I_{SPPA}$ ) of  $30 W/cm^2$  and continuous sonication of 3 min were adjusted to change the local temperature drastically for the better visualization of such a focal point. [Please click here to view a larger version of this figure.](#)

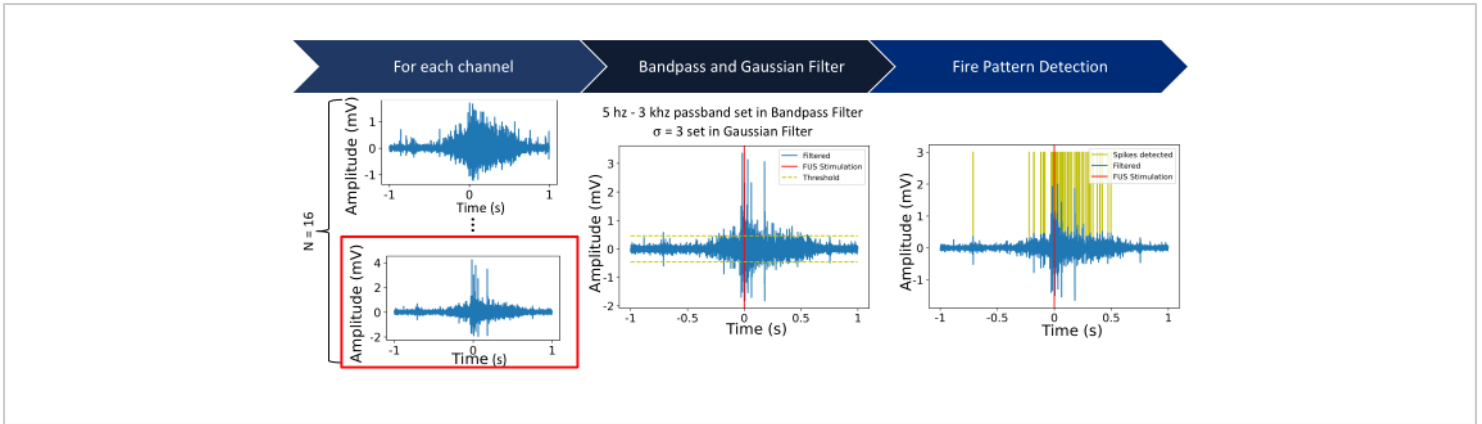


**Figure 5: Processing pipeline.** Step 1: Raw electrical recordings are captured from  $N = 16$  channels. The future steps show the process using channel 16 (outlined in red). Step 2: For each channel, a Butterworth bandpass filter (5 Hz to 3 kHz bandpass) is applied, followed by a Gaussian filter ( $\sigma = 3$ ). A threshold is set as five times the standard deviation of the signal within a 2 s window centered at the start of the sonication. Step 3: Signals above or below the threshold are characterized as spikes. [Please click here to view a larger version of this figure.](#)



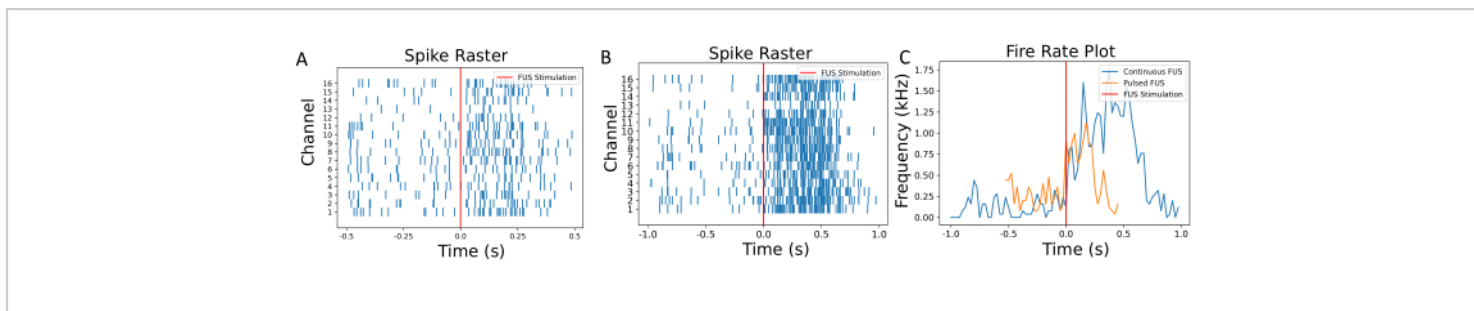


**Figure 6: Raster and firing rate plots.** (A) Raster plot of the detected spikes at each channel as a function of the sonication time. The time of FUS stimulation is annotated using a red line. (B) Raster plot of neurons under different FUS settings with continuous FUS for comparison. (C) The firing rate was calculated using a 50 ms sliding window. The mean firing rates pre- and post FUS neuromodulations were 140 Hz and 786 Hz, respectively. With pulsed FUS, the mean firing rates were 230 Hz and 540 Hz. A shorter activation and less rate change were observed to be induced by this set of varying FUS stimulation. The process for calculating the firing rate is detailed in **Supplementary Figure 1**. [Please click here to view a larger version of this figure.](#)

Parameter	Value
Max Power/Ch.	1.200 W
$P_{\text{actual}}$	0.749 W/channel.
$I_{\text{SPPA}}$	10.79 W/cm <sup>2</sup>
$I_{\text{SPTA}}$	0.05 W/cm <sup>2</sup>
Burst Length	0.100 ms
Frequency	250.00 kHz
Focus	39.800 mm
Period	20.000 ms
Timer	60.000 s

**Table 1: Focused ultrasound (FUS) parameters set on the TPO for the study presented in Figure 4.**

**Supplementary Figure 1: Processing from the Raster plot to the firing rate.**

Step 1: Count the spikes among all the channels to obtain the count number within a given sliding window. Note: Here, a larger sliding window (set to 0.1 s)

was chosen for better illustration. Step 2: Convert the spikes per window length to spikes per second (e.g., here, multiply the counts by 10 to convert to hertz [Hz], and then divide by 1,000 to obtain the value in kilohertz [kHz]). Step 3: The firing

rate curve acquired as a result. An open-source toolkit, along with sampled data, is available on GitHub (<https://github.com/Rxliang/FUSNeuromod>). [Please click here to download this File.](#)

**Supplementary Figure 2: K-wave simulation result temperature profile of LIFU<sup>16</sup>.** Based on the acoustic intensity map shown in **Figure 4**, the K-wave simulation result suggests a maximal temperature increase of 0.04 °C within the center region of the focal zone (radius: 2 mm) using the extreme case of the experimental FUS parameters listed in **Table 1**. [Please click here to download this File.](#)

## Discussion

This manuscript describes a novel method that can be used to record neuronal activity in HiPSCs during FUS neuromodulation. This protocol is generalizable to different FUS transducers and MEA systems. To replicate the results observed with the described protocol, the researcher should ensure that the focal point of the transducer is greater than the area of the bottom of the MEA well. Furthermore, if different neuronal cell lines are used, the filter parameters must be tuned to the expected frequency response for the cells within the well. If representative results cannot be achieved, one should consider modifying the aforementioned parameters (e.g., the burst length, intensity, duty cycle, etc.).

Though this work demonstrated an increase in the firing rate following FUS stimulation, more data must be collected to demonstrate the repeatability of this finding before any conclusions are drawn. This protocol inherits the limitations of MEA systems, which typically have weaknesses stemming from the direct microelectrode current signal recording. Though direct contact with the neuron provides better sensitivity, it may alter the cell and affect the measurement

accuracy. Furthermore, due to the small size of the wells, our system does not include peripheral tissue, which may also play a role in neuromodulation<sup>17</sup>. This may limit the applicability of conclusions drawn from this setup to *in vivo* environments. To study more complex network responses, a higher-channel density MEA system must be designed to improve its sensitivity<sup>18</sup>. Several future directions for this proposed system have been identified, including using a 3D gantry to hold the transducer and ensure accurate placement<sup>19</sup>. Additional improvements could be made regarding the post-processing algorithm, including utilizing a spiking sorting algorithm<sup>20</sup> to classify individual neurons. This process would be beneficial for disentangling the responses of multi-unit neurons in future studies on the mechanisms of FUS. Most importantly, it is essential to incorporate additional modalities of stimulation, such as chemical, electrical, and optical stimuli, to elucidate the underlying mechanisms. These methods can alter neuronal properties and behaviors, such as by inhibiting specific ion channels<sup>15</sup> or modifying the membrane characteristics<sup>21</sup>. By modulating the main factors within the hypothesized signaling pathway, researchers can identify the contributions of each factor in controlled environments and, ultimately, shed light on the complex interactions at play.

Electrical stimulation<sup>22</sup> is one of the most established techniques for neuromodulation, with a long history of successful applications in clinical and research settings. In contrast, FUS and optogenetics<sup>23</sup> are relatively new modalities that have gained attention in recent years. The major advantages of FUS are its non-invasiveness and ability to stimulate neurons at depths that may be difficult to reach with other techniques, including electrical stimulation and optogenetics. However, like optogenetics<sup>24</sup>, FUS has some limitations related to modeling the wave propagation and

associated neuronal responses. Capturing the complexity of tissue's heterogeneous acoustic properties *in vivo* can be challenging, which leads to uncertainties in the pressure field and, consequently, in the neuronal responses. This difficulty in accurately modeling these properties presents a challenge when optimizing the technique for specific real-world applications. The inherent complexities emphasize the importance of *in vitro* systems like the one in this study, as they enable the direct study of responses under controlled acoustic intensity conditions.

In conclusion, this system provides a high-throughput, *in vitro* platform for studying the neuro-modulatory effects of FUS on human neurons. With this system, the mechanisms of action of FUS can be explored by measuring the electrical responses from human neurons when exposed to varying levels and types of stimulation in a controlled environment. Therefore, it offers a valuable supplementary tool to the human and animal models commonly used in the field.

## Disclosures

The authors declare that the research was conducted in the absence of any commercial or financial relationships that could be construed as a potential conflict of interest. Amir Manbachi teaches and consults for BK Medical (GE Healthcare) and Neurosonics Medical and is an inventor on a number of patent-pending FUS technologies. Betty Tyler has research funding from NIH and is a co-owner of Accelerating Combination Therapies (including equity or options). Ashvattha Therapeutics Inc. has licensed one of her patents and she is a stockholder for Peabody Pharmaceuticals.

## Acknowledgments

Amir Manbachi and Nitish Thakor acknowledge funding support from the Defense Advanced Research Projects Agency, DARPA, Award Contract: N660012024075. In addition, Amir Manbachi acknowledges funding support from the Johns Hopkins Institute for Clinical and Translational Research (ICTR)'s Clinical Research Scholars Program (KL2), administered by the National Center for Advancing Translational Sciences (NCATS), National Institutes of Health (NIH). Nitish Thakor acknowledges funding support from the National Institutes of Health (NIH): R01 HL139158-01A1 and R01 HL071568-15.

## References

1. Kamimura, H. A. S., Conti, A., Toschi, N., Konofagou, E. E. Ultrasound neuromodulation: Mechanisms and the potential of multimodal stimulation for neuronal function assessment. *Frontiers in Physics*. **8**, 150 (2020).
2. Manbachi, A., Kempinski, K. M., Curry, E. J. *The Abundant Promise of Ultrasound in Neurosurgery: A Broad Overview and Thoughts on Ethical Paths to Realizing Its Benefits*. SPIE PRESS Bellingham. Washington, USA (2022).
3. Manbachi, A. *Handbook for Clinical Ultrasound. Beginner's Guide to Fundamental Physics & Medical Ultrasound Applications*. Audible. at <<https://www.audible.com/pd/Handbook-for-Clinical-Ultrasound-Audiobook/B0983XJY83>> (2021).
4. Yoo, S., Mittelstein, D. R., Hurt, R. C., Lacroix, J., Shapiro, M. G. Focused ultrasound excites cortical neurons via mechanosensitive calcium accumulation and ion channel amplification. *Nature Communications*. **13** (1), 493 (2022).

5. Szczot, M., Nickolls, A. R., Lam, R. M., Chesler, A. T. The form and function of PIEZO2. *Annual Review of Biochemistry*. **90**, 507-534 (2021).
6. Kim, H. et al. Miniature ultrasound ring array transducers for transcranial ultrasound neuromodulation of freely-moving small animals. *Brain Stimulation: Basic, Translational, and Clinical Research in Neuromodulation*. **12** (2), 251-255 (2019).
7. Hoffman, B. U. et al. Focused ultrasound excites action potentials in mammalian peripheral neurons in part through the mechanically gated ion channel PIEZO2. *Proceedings of the National Academy of Sciences of the United States of America*. **119** (21), e2115821119 (2022).
8. Tyler, W. J. The mechanobiology of brain function. *Nature Reviews Neuroscience*. **13** (12), 867-878 (2012).
9. Collins, M. N., Legon, W., Mesce, K. A. The inhibitory thermal effects of focused ultrasound on an identified, single motoneuron. *eNeuro*. **8** (2), ENEURO.0514-20.2021 (2021).
10. Chalfie, M. Neurosensory mechanotransduction. *Nature Reviews. Molecular Cell Biology*. **10** (1), 44-52 (2009).
11. Launay, P. et al. TRPM4 Is a Ca<sup>2+</sup>-activated nonselective cation channel mediating cell membrane depolarization. *Cell*. **109** (3), 397-407 (2002).
12. Cain, S. M., Snutch, T. P. Contributions of T-type calcium channel isoforms to neuronal firing. *Channels*. **4** (6), 475-482 (2010).
13. Taga, A. et al. Establishment of an electrophysiological platform for modeling ALS with regionally-specific human pluripotent stem cell-derived astrocytes and neurons. *Journal of Visualized Experiments*. (174), e62726 (2021).
14. Taga, A. et al. Role of human-induced pluripotent stem cell-derived spinal cord astrocytes in the functional maturation of motor neurons in a multielectrode array system. *Stem Cells Translational Medicine*. **8** (12), 1272-1285 (2019).
15. Manuel, T. J. et al. Ultrasound neuromodulation depends on pulse repetition frequency and can modulate inhibitory effects of TTX. *Scientific Reports*. **10** (1), 15347 (2020).
16. Treeby, B. E., Cox, B. T. k-wave: Matlab toolbox for the simulation and reconstruction of photoacoustic wave fields. *J. Biomed. Opt.* **15** (2), 021314 (2010).
17. Akhtar, K. et al. Noninvasive peripheral focused ultrasound neuromodulation of the celiac plexus ameliorates symptoms in a rat model of inflammatory bowel disease. *Experimental Physiology*. **106** (4), 1038-1060 (2021).
18. Smirnova, L. et al. Organoid intelligence (OI): The new frontier in biocomputing and intelligence-in-a-dish. *Frontiers in Science*. **1**, 1017235 (2023).
19. Saccher, M. et al. Focused ultrasound neuromodulation on a multi-well MEA. *Bioelectronic Medicine*. **8** (1), 2 (2022).
20. Yger, P. et al. A spike sorting toolbox for up to thousands of electrodes validated with ground truth recordings in vitro and in vivo. *eLife*. **7**, e34518 (2018).
21. Babakhanian, M. et al. Effects of low intensity focused ultrasound on liposomes containing channel proteins. *Scientific Reports*. **8**, 17250 (2018).
22. Liang, R. et al. Designing an Accurate Benchtop Characterization Device: An acoustic measurement platform for localizing and implementing therapeutic ultrasound devices and equipment (amplitude). 2022

---

*Design of Medical Devices Conference, Minneapolis, MN, USA. (2022).*

23. Ko, H., Yoon, S. -P. Optogenetic neuromodulation with gamma oscillation as a new strategy for Alzheimer disease: A narrative review. *Journal of Yeungnam Medical Science.* **39** (4), 269-277 (2022).
24. White, M., Mackay, M., Whittaker, R. G. Taking optogenetics into the human brain: Opportunities and challenges in clinical trial design. *Open Access Journal of Clinical Trials.* **2020**, 33-41 (2020).